ChemCatChem

Research Article
doi.org/10.1002/cctc.202200337

Chemistry Europe
European Chemical Societies Publishing

www.chemcatchem.org

Special Collection

Catalytic Profile Reactor for Multimodal *Operando* Measurements during Periodic Operation

Diego Espinoza[+],[a] Birte Wollak[+],[a] Thomas L. Sheppard,[b, c, d] Ann-Christin Dippel,[e] Marina Sturm,[e] Olof Gutowski,[e] Michael Schmidt,[b] Oliver Korup,[a, b] and Raimund Horn*[a, b]

Multimodal *operando* measurement concepts aim to provide structure-activity relations of heterogeneously catalyzed reactions during operation. While the utilization of multiple characterization and spatiotemporally-resolved techniques provides complementary information at relevant time and length scales, different reactor operation modes allow to track catalyst dynamics. However, combining these measurement concepts require complex experimental setups with high demands from a strongly interdisciplinary field of reaction engineering, physics and chemistry. In this study, a fully automated and integrated catalytic profile reactor setup is introduced which is capable of measuring spatiotemporally-resolved species concentration, temperature and catalyst structure information under periodic reaction conditions. The oxidative dehydrogenation of C_2H_6 to C_2H_4 over MoO_3/γ-Al_2O_3 was used as a test system. Using the periodic profile approach, the catalytic system was investigated through activity measurements resolved in time and space combined with reactor simulations and *operando* high-energy X-ray diffraction. The presented catalytic profile reactor setup is a versatile technology, aiming to promote combined and detailed analysis of local catalyst activity and structure, for improved reproducibility and quality of *operando* measurements.

Introduction

The use of renewable energies and raw materials is essential for a successful energy transition away from finite natural resources.[1] However, the highly alternating energy supply resulting from sustainable sources represents a major challenge for established catalytic processes, which are predominantly run at an optimum operation point in steady state. Solution concepts consider storage or buffer tanks to compensate for alternations in reaction feed. A more innovative approach consists of novel catalysts and reactor concepts capable of being operated at dynamic reaction conditions.[2] To develop such innovative catalytic processes, gaining a fundamental understanding of catalyst structure-activity relations is an essential step. The field of *operando* research evolved to meet this challenge, aiming to unravel catalyst structure-activity relationships through detailed modeling[3,4] and multimodal experimental approaches.[5]

Operando measurement concepts in catalysis combine catalytic activity measurements (e.g. gas and temperature analysis) with structural characterization (e.g., X-ray diffraction (XRD),[6] X-ray absorption spectroscopy (XAS),[7] X-ray emission spectroscopy (XES),[8,9] etc.) during operation, thus in the actual working state of the catalyst. To harvest as much relevant and complementary information as possible, multimodal *operando* measurement concepts aim to cover broad space and time scales, and combine multiple characterization techniques within the same reactor.[9,10]

Spatially-resolved techniques are now implemented as a relatively common tool in *operando* catalysis research, providing localized information throughout the entire catalyst bed. However, simultaneous measurement of local catalytic activity and catalyst structure information involves high experimental complexity, requiring to insert a gas sampling device (e.g., capillary sampling technique) in the catalyst bed, and at the same time to make the reactor bed optically accessible for various characterization techniques. As a result, most studies measure either catalyst activity[11] or catalyst properties[12] in a

[a] *D. Espinoza,[+] B. Wollak,[+] Dr. O. Korup, Prof. Dr. R. Horn*
Institute of Chemical Reaction Engineering
Hamburg University of Technology
Hamburg 21073 (Germany)
E-mail: horn@tuhh.de
Homepage: www.crt.tuhh.de/index.php/Prof._Dr._R._Horn
[b] *Dr. T. L. Sheppard, M. Schmidt, Dr. O. Korup, Prof. Dr. R. Horn*
REACNOSTICS GmbH
Hamburg 20457 (Germany)
[c] *Dr. T. L. Sheppard*
Institute for Chemical Technology and Polymer Chemistry
Karlsruhe Institute of Technology
Karlsruhe 76131 (Germany)
[d] *Dr. T. L. Sheppard*
Institute of Catalysis Research and Technology
Karlsruhe Institute of Technology
Eggenstein-Leopoldshafen 76344 (Germany)
[e] *Dr. A.-C. Dippel, Dr. M. Sturm, O. Gutowski*
Deutsches Elektronen-Synchrotron DESY
Hamburg 22607 (Germany)
[+] *These authors contributed equally in this work.*

Supporting information for this article is available on the WWW under https://doi.org/10.1002/cctc.202200337

This publication is part of a joint Special Collection with ChemElectroChem on "Catalysts and Reactors under Dynamic Conditions for Energy Storage and Conversion (DynaKat)". Please check our "homepage for more articles in the collection".

spatially-resolved manner, hence addressing only one side of the chemical system in a given experiment.

Few studies have demonstrated the strength of combined spatially-resolved catalyst activity and characterization measurements e.g. coupled to Raman-spectroscopy[13] or XAS.[14,15] Two reactor systems were utilized in synchrotron radiation studies for this purpose, the spatially resolved capillary inlet reactor system for fixed beds combined with XAFS (here denoted as SPACI-FB-XAFS) and the Compact Profile Reactor (CPR). To correlate reliably structure-activity using such *operando* reactor systems, precisely controlled reaction parameters (e.g., temperature, pressure, concentration, flow velocity) are required, following plug flow behavior without significant radial gradients, channeling, bypass flows and dead volumes. This is of particular importance in spatial profiling techniques that produce radially averaged data in axial direction of the catalyst bed, which are only meaningful if plug flow assumptions are valid and reaction parameters are carefully monitored along the whole measurement range. The SPACI-FB-XAFS system applies one hot air blower for heating a larger sample (inner diameter 4 mm), which is shown by Newton et al.[16] to be problematic as it can easily result in temperature gradients, resulting in non-uniform process conditions. In contrast, the Compact Profile Reactor (CPR) utilizes a direct heating between the sample and an oven, enabling a uniformly heated catalyst bed length of up to 6 cm. Highly beneficial in *operando* catalysis studies, in particular at synchrotron radiation facilities, is the high setup automation degree and the compact reactor design, which allows for quick setup assembly and straightforward operation. This was demonstrated in a combined spatially-resolved *operando* study using XAS.[15] In addition, the power of spatial profiling for fast kinetic model development by fitting complete reactor profiles was shown previously. The kinetic model includes the catalyst oxidation state as catalyst property and was validated with experimentally observed oxidation states.

The synergy between spatially-resolved catalyst activity data and theoretical investigations through the development and validation of more detailed models[4,17] or CFD simulations[18] was demonstrated in several studies. Future detailed model approaches (e.g., *operando* modeling) require catalyst information at dynamic reaction conditions, revealing transient gas species and dynamic structural changes. Besides this, operating catalytic reactors at varying reaction conditions becomes more relevant with regards to future demands on catalysts, evaluating catalytic performance at an averaged optimum obtained at transient conditions.[2] One way to operate the reactor at dynamic reaction conditions is to periodically modulate inlet feeds or temperatures. While periodic reactor operation combined with simulations and traditional in- and outlet gas analysis has been extensively studied with the aim of enhancing catalytic performance,[19] spatially-resolved periodic profiling in *operando* measurements is relatively unknown. The combination of periodic reactor operation with spatially-resolved *operando* techniques require to add another domain in time, using time-resolved gas, temperature and structural analysis. This increases experimental complexity further. However, such data would have high potential for validation and development of improved kinetic models and to promote systematic knowledge-based optimization of catalysts at varying reaction conditions.

In order to provide such data sets, the aim of this study is to develop systematically the spatiotemporally-resolved operando profile methodology under dynamic reaction conditions. The oxidative dehydrogenation of ethane to ethylene (ethane ODH) over a $MoO_3/\gamma\text{-}Al_2O_3$ catalyst was chosen as test system. While this system represents a rather simple model system, the reaction belongs to the prominent class of selective oxidation reactions over transition metal oxide catalysts. This reaction class faces the major challenge to produce alkenes and oxygenates selectively, i.e. avoiding total combustion reactions.[20] To overcome the selectivity problem, the development of highly selective catalysts[21] and exploring alternative reactor operation modes[2,22] play a decisive role. For example, periodic reaction conditions aim to stimulate favorable oxygen species that accelerate the desired reaction pathway based on Haber's concept of different oxygen species.[23,24] The reaction is usually described by the Mars-van Krevelen (MVK) mechanism,[24,25] in which all hydrocarbon reactions occur via lattice oxygen and the catalyst participate actively by undergoing cycles of oxidation and reduction. The distinct catalyst dynamics in performance and structure as well as the structural reversibility as function of the reaction environment of such catalytic system is particular advantageous for developing the introduced methodology. Additionally, the test chemical system is stable with time on stream and relatively well-studied.

In this work, the CPR was operated periodically, using a sinusoidal feed inlet. Catalytic performance was investigated through measured concentration profiles combined with kinetic modeling. The latter was used for a systematic catalytic performance study over a wide periodic parameter range. Using this approach of periodic profile reactor operation, the catalyst structure was studied by *operando* spatiotemporally-resolved high-energy XRD at the PETRA III synchrotron light source. The introduced CPR setup is a novel tool for versatile multimodal measurements, optimized for combined spatiotemporally-resolved *operando* measurements under dynamic, uniform and well-defined reaction conditions.

Results and Discussion

Periodic profile reactor simulations

In a previous study by the authors,[15] spatially-resolved concentration profiles obtained at a constant inlet feed were used for the fast development of a steady state kinetic model. The previous study was performed with the same reactor system (CPR, see Figure 13) and catalytic test system, i.e. ODH of ethane to ethylene over a 30 wt% $MoO_3/\gamma\text{-}Al_2O_3$ catalyst [Equation (1)], as in this work.

$$C_2H_6 + 0.5\ O_2 \rightarrow C_2H_4 + H_2O \quad (1)$$

The kinetic model follows the MVK mechanism and considers, apart from the main ODH reaction, partial and total combustion reactions of C_2H_6 and C_2H_4 to CO_x as well as the reoxidation of the catalyst by gas phase O_2. Notably, the kinetic model considers the oxidation state of molybdenum as catalyst property, referred to θ_{ox}. For a detailed description the reader is referred to the supporting information section.

Based on this model, a transient reactor model was developed which allows to perform profile reactor simulations with periodically modulated inlet concentrations. Periodic parameters include phase amplitude (PA), phase length (PL), and phase shift (PS), exemplified for oxygen with 10% PA (O_2 inlet flow rate 3 ± 0.3 ml/min) and 60 s PL in Figure 1. Here, the periodic oxygen profile in molar flow rate during ethane ODH was simulated as a function of position within a 32 mm long catalytic fixed-bed and as function of time over five minutes per sampling position.

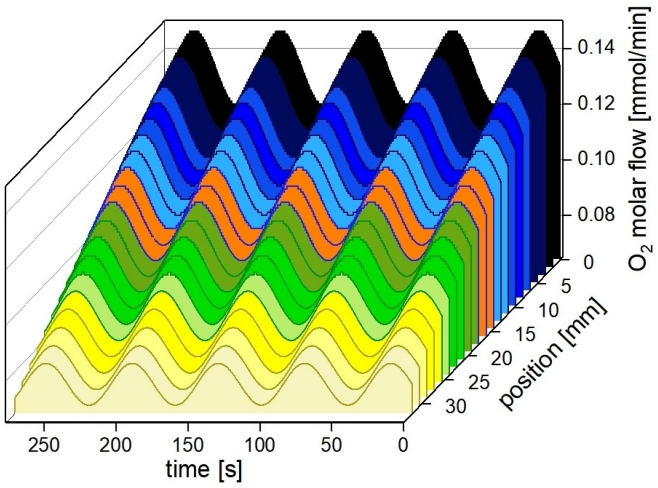

Figure 1. Simulated periodically modulated oxygen concentration profile as function of position along the catalyst bed and time. Simulation conditions: Inlet composition C_2H_6/O_2:10/10, ethane PA 10%, oxygen PA 10%, PL 60 s, PS 180°, 515 °C, 1 bar, OD 6.0 mm/ID 4.0 mm, 32 mm catalyst bed, 30 ml/min, 30 wt% MoO_3/γ-Al_2O_3.

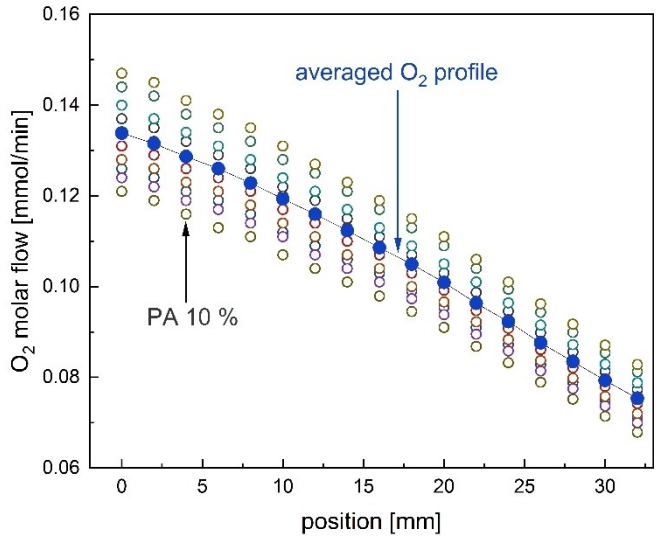

Figure 2. Simulated oxygen concentration periodically modulated as function of position along the catalyst bed. Blue circles: Simulated oxygen concentration averaged through time per position. For illustration purpose only, the number of simulated points in time and position were reduced. Simulation conditions: Inlet composition C_2H_6/O_2:10/10, ethane PA 10%, oxygen PA 10%, PL 60 s, 515 °C, 1 bar, OD 6.0 mm/ID 4.0 mm, 32 mm catalyst bed, 30 ml/min, 30 wt% MoO_3/γ-Al_2O_3.

Using this simulative periodic profile approach, spatiotemporally-resolved reactor data are obtained, providing transient process information of the gas phase within an additional information domain in time, compared to spatially-resolved profile data at steady state, which reveal relevant information solely in space.

In order to compare catalytic performance in terms of selectivity and conversion between profile runs in steady state and periodic conditions, a standardized profile data treatment was used. Figure 2 illustrates the data treatment for the periodic oxygen concentration profile previously shown in Figure 1.

Here, the oxygen profiles varying periodically in time are projected onto the spatial coordinate. In consequence, unlike profile data obtained at steady state, periodic data have a flow rate range for one or more reactants, dependent on the applied PA, at each position in the catalyst bed. Through combinations of reactants with different PA and PS a wide condition range can be scanned within one profile. Experimentally, the periodic profiling concept reduces the experimental workload required for the same information, as compared to steady state spatial profiling or the traditional effluent approach. A representative flow rate at each position is obtained by calculating the average through the sampling time per position (blue circles, Figure 2). All concentration profiles in this work, simulated or measured, are further shown as averaged profile data.

Figure 3 shows an overview of simulated steady state and periodic concentration profiles (PA 10%, PL 60 s, PS 180°) for all components occurring in the ODH reaction mixture in the presence of gas phase oxygen. The reactants ethane and oxygen are consumed up to a conversion level of $X_{C2H6} = 30\%$ and $X_{O2} = 43\%$. Ethylene is formed as desired product [Equation (1)], while the main byproducts are water, carbon monoxide, and carbon dioxide in small quantities. All components show a complete match with no difference in between different reactor operations.

In order to explore potential differences, a wide range of periodic parameters and combinations of PA 5–35%, PL 0.01–60 s, and PS 0–180° were tested using a parametric sweep. Here again, no difference in catalytic performance could be tracked.

This system response is interesting because, when observing the form of the rate law equations, is possible to notice that the model descriptor θ_{ox} (see supplementary Equation S3) introduces non-linearity on the equation system. Therefore, when a perturbance is applied to the reactor, in this case by means of a periodically modulated feed around its steady state value, a mean value concentration different from the steady state is to be expected. However, as can be seen in Figure 3, this is not the case.

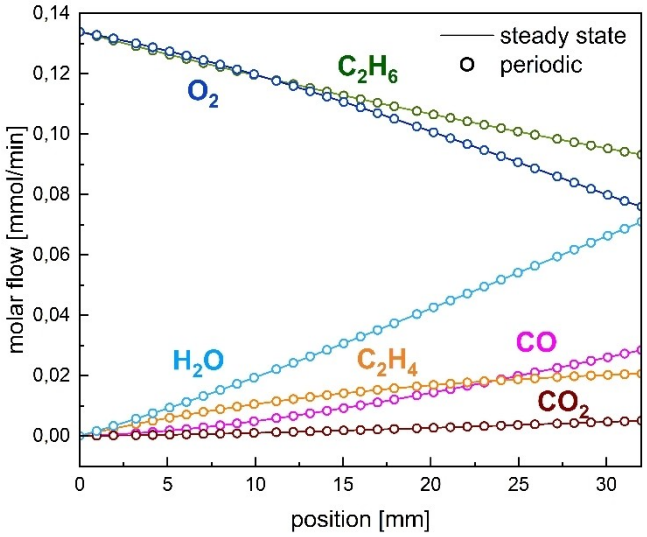

Figure 3. Simulated steady state and averaged periodic profiles for the reactants (ethane, oxygen), target product (ethylene), byproduct (water), and undesired byproducts (carbon monoxide, carbon dioxide). Simulation conditions: Inlet composition C_2H_6/O_2:10/10/80, ethane PA 10%, oxygen PA 10%, PL 60 s, PS 180°, 515 °C, 1 bar, OD 6.0 mm/ID 4.0 mm, 32 mm catalyst bed, 30 ml/min, 30 wt% MoO_3/γ-Al_2O_3.

In our previous study, it was demonstrated with the help of XANES that the catalyst's average bulk oxidation state is rather stable and close to MoO_3 even when the partial oxygen pressure declines rapidly along the bed. This characteristic of the catalytic system is described as well by the model descriptor θ_{ox}, where $\theta_{ox} = 1$ represents the catalyst in its fully oxidized state (MoO_3), while for $\theta_{ox} = 0$, the catalyst is in the reduced state (MoO_2). Since under oxidative conditions, the catalyst changes barely its oxidation state, hence the term θ_{ox} is rather constant and close to the unity, the entire system behaves linearly. And thus, the response obtained in the simulations.

The linearity of the reaction system combined with the CPR as a kinetically well-defined spatial profile test reactor is optimal to develop an experimental methodology for spatiotemporally-resolved periodic profiling. Such measurement methodology presents an essential counterpart to reactor simulations, required for validation of the transient model results and further (detailed) model development. To illustrate this point, linearity of the reaction system results in unchanged catalytic performance under periodic conditions or at steady state. Furthermore, the CPR follows plug flow behavior, considering only species gradients in axial direction with no additional transport effects. This assumption was validated by fulfilling the criteria presented by Mears[26] (see supplementary Equation S10). Thus, all experimentally observed changes in catalytic performance should originate from the setup, which allows distinct error identification. This makes a sophisticated method development feasible.

Periodic profile reactor experiments

The CPR reactor operation was adapted from steady state to a fully automated periodic mode, allowing to dose reactant inlet concentrations periodically in a flexible manner and related to each other. In order to ensure proper working of all periodic parameters, functionality tests in an empty reactor tube were performed to analyze the periodic variable response with the used mass flow controllers (MFCs) and reactor control system. Results obtained are given in Figure 4, showing the molar flow rates of oxygen at different PA (Figure 4a), PL (Figure 4b), and PS referred to ethane (Figure 4c). A good linear control and

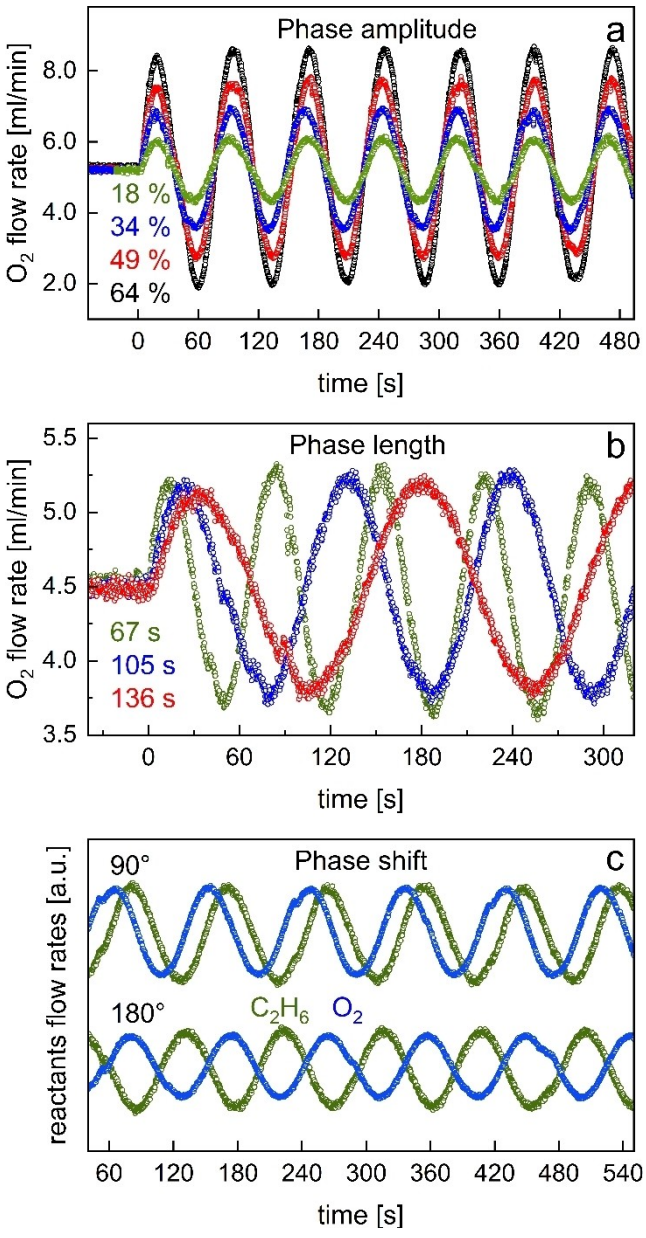

Figure 4. Functionality test results of periodic variables. a) PA 18, 34, 49, and 64% using oxygen; b) PL 67, 105, and 136 s using oxygen; c) PS 90 and 180° using ethane and oxygen. Reaction conditions: 25 °C, 1 bar, OD 6.0 mm/ID 4.0 mm, 40 ml/min, empty reactor outlet measurement.

symmetrical oscillation behavior for all periodic variables throughout the investigated parameter range is observed. The inert flow was utilized to compensate for changes in the total flow rate resulting from the periodically fluctuating species. The extreme case represents two components varied in phase with large PA 57% that reveals a total flow rate deviation of up to 6%. Thus, further improvement of the control system to keep the total flow rate constant at high PA and low PS is necessary and will be the focus of future work. Overall, reliable periodic operation of the CPR for further tests under reaction conditions was confirmed.

In order to follow the periodic signal for ethane (main reactant) and ethylene (main product) during ethane ODH precisely, the two corresponding mass to charge ratios were scanned (m/z: C_2H_6 (30), C_2H_4 (27)). A periodic profile measurement was conducted through a 40 mm long catalyst bed, fluctuating oxygen with a PA of 5% and ethane with 9% at PL 9 s and PS of 180° shifted to each other. Figure 5a shows the ethane and ethylene concentration profiles as function of time at the beginning (0 mm), at four positions within (8, 16, 24, 32 mm), at the end (40 mm), and downstream the catalyst bed. Periodic profile data demonstrate stable operation at reaction conditions, allowing for reliable correlation of catalytic performance between steady state and periodic conditions.

In Figure 5b the corresponding averaged periodic and steady state concentration profiles as function of position within the catalyst bed are presented. A good match is shown for ethylene. Minor deviations are observed for ethane with a maximum at position 32 mm, corresponding to a conversion difference of 2.3% in between steady state and periodic profiles. This is in the accuracy range of the MS, determined by evaluating observed deviations over one day, as well as by several replicate profiles shown in a previous study.[15] Profile results reveal stable catalytic performance with no significant difference at periodic conditions compared to steady state, complementing simulative profile results obtained by the kinetic model shown above. Additional experiments could be conducted, which test the range beyond the steady state conditions, extending the given model validity range towards higher oxygen and ethane conversion levels, and different inlet concentrations. However, due to the linear behavior no pronounced deviations are expected during extrapolations.

Overall, the introduced periodic profile methodology using the CPR demonstrates reliable operation for both operation modes. This allows efficient and systematic catalyst performance investigations at dynamic reaction conditions, finding optimization potential or lowered catalyst performance over broad conversion ranges in short times. The CPR allows further to deduce pure kinetics of various chemical systems at dynamic reaction conditions decoupled from transport effects, required for any reactor design and simulation (see supplementary Table S4). Since catalytic performance is inseparably linked to the catalyst structure, results shown so far display only one part of the chemical system, covering transient chemical processes occurring in the gas phase. For achieving a holistic picture of the catalytic system, spatial and temporal structural information of the catalyst at dynamic reaction conditions are essential, which is focus in the spatiotemporally-resolved *operando* XRD section.

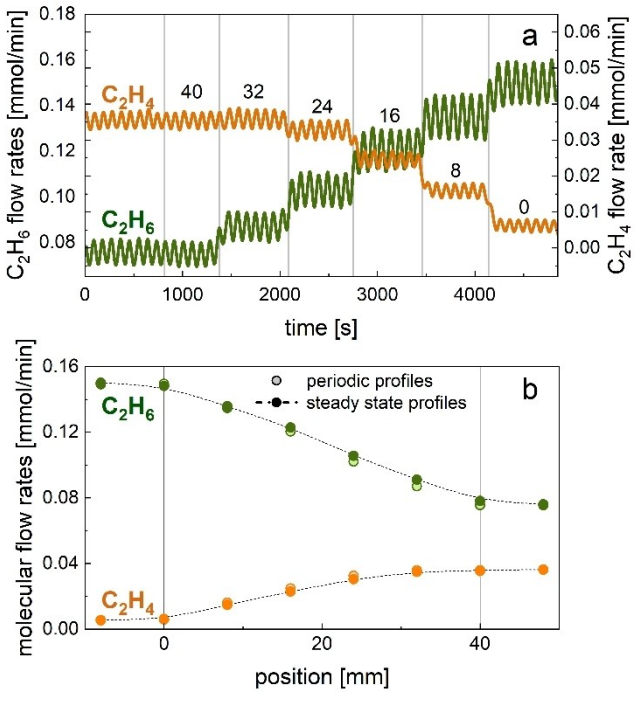

Figure 5. Measured periodic (CP_PP) and steady state (CP_SS) species concentration profiles for ethane and ethylene through the catalyst bed during ethane ODH. a) Concentration profiles as function of measurement time acquired at six sampling positions (0, 8, 16, 24, 32, 40 mm) along the entire catalyst bed. b) Averaged concentration profiles as function of the catalyst bed position. Reaction conditions: Inlet composition C_2H_6/O_2:10/10, ethane PA 9%, oxygen PA 5%, PL 95 s, PS 180°, 530 °C, 1 bar, OD 6 mm/ID 4.0 mm, 40 mm catalyst bed, 40 ml/min, 30 wt% MoO_3/γ-Al_2O_3.

Periodic *operando* temperature profiles

Temperature has a strong influence on reaction kinetics and is therefore an essential measurement parameter. The capillary measurement technique allows to measure the temperature in the center and in longitudinal direction of the catalyst bed. In combination, the CPR control system enabled to follow periodic temperature response precisely by recording temperature information every second as function of position within the catalyst bed. During *operando* experiments six profile runs were performed, simultaneously measuring local gas composition, temperature and XRD. One profile was obtained at steady state (1_SS) and two at periodic (3_PP, 5_PP) conditions. One replicate profile was recorded for each measurement (2_SSR, 4_PPR, 6_PPR), comprising six profiles in total (see experimental section). The number in the profile runs from 1 to 6 denote the sequence in which the profiles were recorded within the total measurement time of 28 h. Notably, *operando* experiments were run until full oxygen conversion, in contrast to a maximum oxygen conversion level of 60% in the catalytic performance studies (see previous sections). An overview of the averaged temperature profiles from all six profile runs is given in

Figure 6a. The catalyst bed begins at position 0 and ends at 36 mm, denoted with black lines. The periodic inlet temperatures (512 °C, 0 mm) show a good match to each other with a slightly lower inlet temperature than the steady state profiles (513 °C, 0 mm). Further, the overall profile shapes of all runs are in good agreement with no significant differences between the two operation modes. The temperature increases by 12 °C until position 14 mm and the subsequent temperature decline forms a small hot spot at position 14 mm. In this bed range more than 80% of oxygen is converted with full conversion reached at position 18 mm, revealed by the simultaneously measured oxygen concentration profiles. At this position, catalytic performance changes from strongly exothermic oxidation reactions consuming gas phase oxygen to endothermic reactions such as steam reforming. In combination, exothermic oxidation reactions releasing heat dominate. *Operando* gas temperature profiles compare well with the profiles results from the previous sections, as well as with studies performed in earlier work.[15]

While the averaged temperature profiles are very similar, non-averaged temperature profiles reveal a notable non-linear response behavior. Figure 6b shows the periodic temperature profile (3_PP) as function of time, demonstrating a sine wave response with a different amplitude at nine positions within the catalyst bed from 0 to 16 mm. At the beginning of the catalyst bed (0 mm) the temperature oscillates with a very small amplitude (±1 °C), most likely originating from a changing thermal conductivity of the feed reaction mixture. The magnitude amplifies reaching 9 °C at 16 mm due to increasing reaction progress along the axial position of the catalyst bed. At the positions 14 and 16 mm the sine wave shows a non-symmetrical oscillation with mostly constant phase minima in between 12–14 mm, as consequence of high oxygen conversion levels. The observed temperature pattern is a complex combination of local transport phenomena and local chemical reactions. In order to fully understand the nature of this behavior a more detailed model approach would be required which is beyond the scope of the present work, for example using a heterogeneous reactor model.

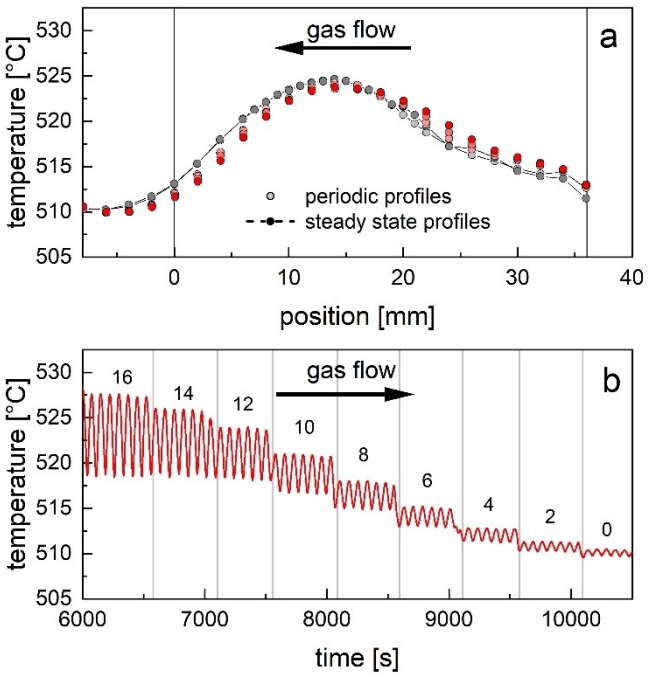

Figure 6. Periodic and steady state temperature profiles measured *operando* during ethane ODH *at* beamline P07, PETRA III (Hamburg, Germany). a) Averaged temperature profiles as function of the catalyst bed position along the entire catalyst bed of all six profile runs. b) Temperature profile as function of measurement time corresponding to the periodic profile run 3_PP at 9 positions within the catalyst bed. Reaction conditions: Inlet composition C_2H_6/O_2:10/10, 510 °C (−6 mm), 1 bar, OD 6 mm/ID 5.6 mm, 38 mm catalyst bed, 15 ml/min, 30 wt% MoO_3/γ-Al_2O_3. Averaged periodic profiles: 3_PP/4_PPR: PA 15%/PL 93 s, 5_PP/6_PPR: PA 38%/PL 91 s.

Spatiotemporally-resolved *operando* XRD

The periodic profiling methodology utilizing the CPR was further developed for combined spatiotemporally-resolved *operando* high-energy XRD to explore structural characteristics of the MoO_3/γ-Al_2O_3 catalyst during ethane ODH. The Corresponding temperature profiles, simultaneously measured with XRD, are focus in the previous section. Corresponding concentration profiles compare well to profiles obtained in the previous catalyst performance sections. Therefore, the following section will only focus on the spatially-resolved XRD profiles.

XRD experiments were carried out at beamline P07 (PETRA III, DESY), comprising six profile runs in total. Each profile run contains background features (e.g. the fused silica reactor) which should remain unchanged throughout all profiles conducted within the same reactor tube. Comparing the same measurement positions between different profile runs allows to evaluate operation stability of the beamline and reactor. Figure 7 shows normalized patterns of all profiles acquired of the empty reactor tube (Figure 7a, −10 mm, OD 6.0 mm/ID 5.6 mm), close to the catalyst bed (Figure 7b, −2 mm), and at the start of the bed (Figure 7c, 0 mm). The fused silica reactor tube shows characteristic signal contributions with a broad signal in the q range of 1.2–2 $Å^{-1}$ (Figure 7a). A good match between all patterns at this position is observed, confirming stable beamline operation over the whole measurement time of 28 h. Quartz wool plugs were used to fix the catalyst bed in position, resulting in a short zone where mixing between quartz wool and catalyst particles is observed. By shaping the beam size to 0.5×0.5 mm^2 on the sample, minor reflections from the catalyst therefore appeared at −2 mm in all profile runs (Figure 7b). This information should be considered when evaluating initial slopes of species concentration profiles. Diffractograms obtained at position 0 mm (Figure 7c) show pronounced catalyst signals compared to positions before, indicating that the beam is fully positioned within the catalyst bed. Therefore, this position is assigned to the beginning of the catalyst bed. Notably, the patterns recorded at the same position (−2 or 0 mm) show significant changes in total intensities (e.g. 1.64 $Å^{-1}$, 1.92 $Å^{-1}$) and signal to background ratios, which is related to changes of the catalyst structure with time and discussed in more detail later in this section.

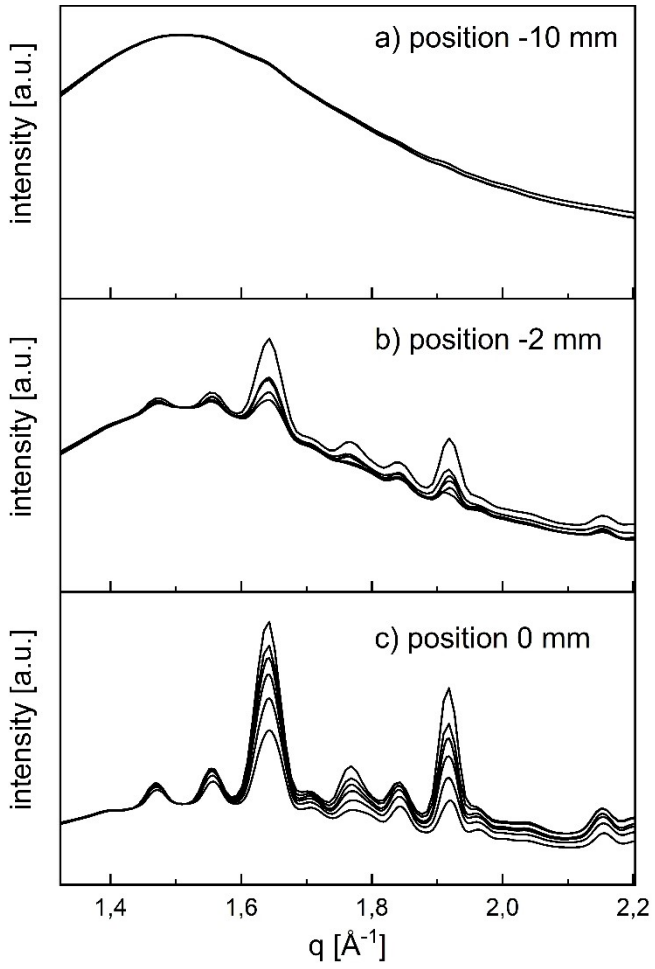

Figure 7. XRD patterns of all profile runs at three different positions measured *operando* at beamline P07, PETRA III (Hamburg, Germany) over 28 h. a) Empty reactor tube (position −10 mm); b) Mixture of catalyst particles and quartz wool close to the beginning of the catalyst bed (position −2 mm); c) Beginning of the catalyst bed (position 0 mm). Diffractograms are normalized to the maximum of the fused silica signal at 1.5 Å^{-1}.

However, the pronounced change between patterns acquired at the transition zone (Figure 7b) and the beginning of the bed (Figure 7c) is reproducible between all profiles, confirming that the same sample volume was probed in each profile. This demonstrates precise and stable motor positioning of the spatial profile reactor, as well as negligible impact of the spatial profiling methodology caused by repetitive moving of the sampling capillary through the center of the catalyst bed. For example, the latter could have led to particle attrition and densification of the bed, which would have shifted the start position of the catalyst bed down in the vertically positioned tube. This should be considered with care when using capillary sampling in catalyst materials, which may have low mechanical stability. A densification of the catalyst bed could result in different catalyst mass per sample position with strong impact on species concentration profile measurements and hence, on catalytic performance observations and deduced kinetic parameters. Overall, the XRD results complement observations made in a previous XAS study, demonstrating long-term stability and reproducibility of the profile measurement technique with the CPR and the used reaction systems, addressed by evaluating concentration profiles using a statistically well-defined experimental design plan.[15]

During periodic reactor operation, XRD scans were performed with short acquisition times of 1 s over three minutes per position. Corresponding spatiotemporally-resolved XRD results are exemplarily shown for 3_PP in Figure 8 at three sampling positions within the catalyst bed, illustrated in green (0 mm), yellow (20 mm), and blue (36 mm).

At each position seven patterns with a time interval of 30 s are presented. When each pattern was acquired, the catalyst was exposed to a different gas composition. These diffractograms, as the case for all periodic profiles, show no change in time per sampling position, suggesting stable catalyst bulk structure over the applied time periods and conditions. In our previous work,[14] this reaction system could be described by a MVK mechanism, which considers the participation of lattice oxygen. The observations of an unchanged bulk structure and average catalytic performance under periodic reaction conditions compared to steady state indicates that the exchange between lattice and gas phase oxygen is fast and restricted to a near-surface region of the catalyst.

While time-resolved XRD shows a constant catalyst bulk structure over short time ranges, distinct structural changes are observed spatially-resolved along the catalyst bed, comparing position 0, 20, and 36 mm (Figure 8).

Structural changes in the profile were induced by running the reaction until full oxygen conversion, whereby the catalyst

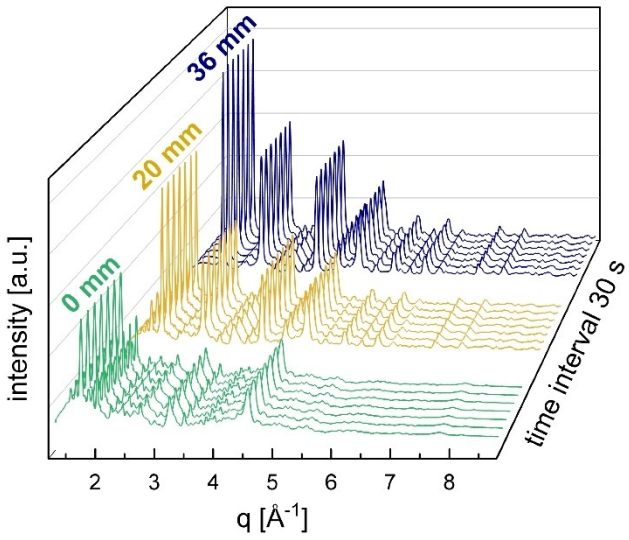

Figure 8. Time-resolved XRD patterns measured *operando* during ethane ODH at beamline P07, PETRA III (Hamburg, Germany) at periodic reactor operation (3_PP). Patterns at three positions within the catalyst bed, illustrated in green (0 mm), yellow (20 mm), and blue (36 mm), acquired with a time interval of 30 s within a measured time range of 180 s are shown. Diffractograms are normalized to the maximum intensity reflection, respectively. Reaction conditions: Inlet composition C_2H_6/O_2:10/10, PA 15%, PL 93 s, 515 °C, 1 bar, OD 6.0 mm/ID 5.6 mm, 38 mm catalyst bed, 15 ml/min, 30 wt% MoO_3/γ-Al_2O_3, profile time span 3 h, exposure time 1 s. Beamline P07: Beam size 0.5×0.5 mm^2 (h×v), 103.413 keV (λ = 0.1199 Å).

undergoes reduction and corresponding crystallographic phase changes. To compare periodic with steady state XRD profile results, time-resolved XRD patterns were averaged per position. An overview of the obtained averaged spatially-resolved XRD profiles along the entire reactor, corresponding to 3_PP, is presented in Figure 9. The periodic XRD profile has 19 sampling points, scanned with a sampling point density of 2 mm along the catalyst bed (0–36 mm). Three sections can be distinguished in the catalyst bed. In the first section from 0–18 mm, the patterns look very similar with respect to the occurring reflections, while signal to background ratio and the peak intensities vary, e.g. an increasing relative intensity of the reflection at 1.64 $Å^{-1}$. During ethane ODH oxygen defects are induced and in turn, the catalyst is partially reduced. Such lattice perturbations are compensated by forming various non-stoichiometric molybdenum intermediate oxides with different metal to oxygen ratios.[27,28] Therefore, we assume a mostly stable phase mixture of various molybdenum oxides, such as MoO_3 [ICDD No-. 98-064-4065], MoO_2 [98-008-0830], Mo_8O_{23} [ICDD No-. 98-020-2203], Mo_4O_{11} [ICDD No-. 98-002-4033], Mo_9O_{26} [ICDD No-. 98-003-8014], $Mo_{17}O_{47}$ [ICDD No-. 98-002-8333], $Al_2Mo_3O_{12}$ [ICDD No-. 98-008-8903], with their strongest reflections present in the lower q range of 1.4–2 $Å^{-1}$. Extensive peak overlap of the reflections of the numerous low-symmetry MoO_{3-x} phases make a reliable qualitative phase identification challenging. In the second section, catalyst reduction can be precisely followed through a pronounced phase transformation from the previous molybdenum (sub-)oxide phase mixture towards a highly crystalline MoO_2 phase (18–24 mm). Downstream of position 24 mm, in section three, all patterns are essentially identical until the end of the catalyst bed (24–36 mm). Periodic XRD profile results compare well with the steady state XRD profile in terms of the main features, showing the same catalyst bed regimes and chemical reduction. Figure 10 shows exemplarily the formed crystalline MoO_2 phase (third regime), assigned to a monoclinic crystal structure ([ICDD No-. 98-015-2316), obtained from 1_SS and 3_PP. The periodic profile 3_PP was recorded 16 h after the steady state profile 1_SS in which the reactor was operated continuously at a high temperature of 515 °C.

Both patterns match well in terms of the characteristic reflections and peak shape throughout the entire scanned angular range and demonstrate high data quality enabling a thorough structure analysis for example by Rietveld refinement. However, noticeable discrepancies in the signal to background ratio are observable (e.g. 1.82, 2.58, 3.66 $Å^{-1}$, etc.) at an obviously constant full width at half maximum (FWHM), respectively. This suggests a growing number of MoO_2 crystals, which is related to continuous catalyst reduction with time.

This observation of continuous catalyst reduction at larger time scales is further seen by comparing patterns of different profile runs, whether conducted at steady state or periodic conditions, obtained at the same sampling position in the first bed regime (0–18 mm). Figure 11 shows the relevant q region of 1.4–2 $Å^{-1}$ from (averaged) patterns of all profile runs measured at position 16 mm. The reflection at 3.15 $Å^{-1}$ originates from the γ-Al_2O_3 support, which is expected to remain unchanged over all profiles at the same sampling position and was thus used for intensity normalization. By means of normalization, patterns at the same sampling position

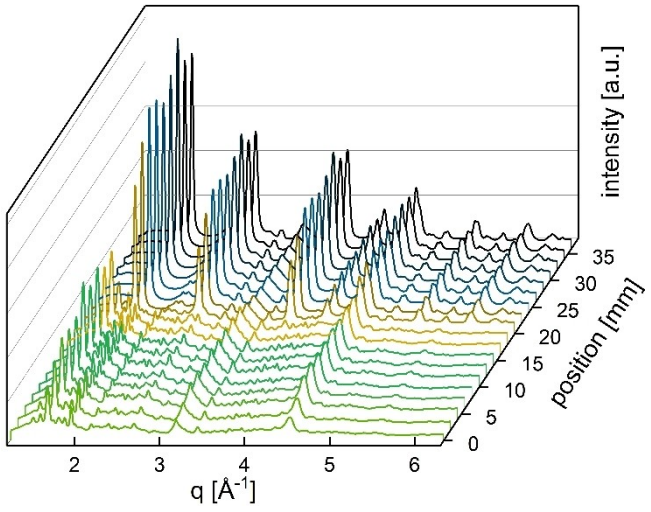

Figure 9. Averaged spatially-resolved XRD profile (3_PP) measured *operando* during ethane ODH at periodic reactor operation at beamline P07, PETRA III (Hamburg, Germany). Yellow colored patterns (18–24 mm) mark the catalyst bed range where the catalyst undergoes reduction with distinct phase transformations. Reaction conditions: Inlet composition C_2H_6/O_2:10/10, PA 15%, PL 93 s, 515 °C, 1 bar, OD 6 mm/ID 5.6 mm, 38 mm catalyst bed, 15 ml/min, 30 wt% MoO_3/γ-Al_2O_3, profile time span 3 h, XRD exposure time 1 s, 180 patterns averaged. Beamline P07: Beam size 0.5×0.5 mm^2 (h×v), 103.413 keV (λ = 0.1199 Å).

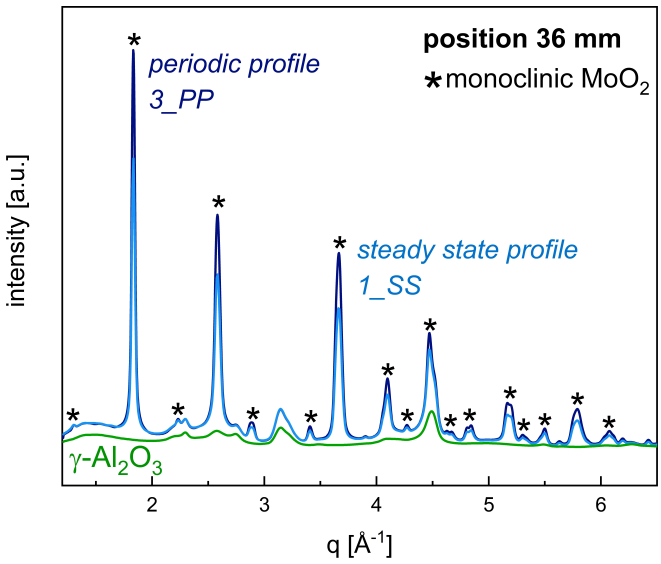

Figure 10. Averaged XRD patterns measured *operando* at position 36 mm under periodic (3_PP) and steady state (1_SS) reaction conditions. Diffractograms are normalized to the maximum fused silica signal at 1.4 $Å^{-1}$, respectively. Reaction conditions: Inlet composition C_2H_6/O_2:10/10, 515 °C, 1 bar, OD 6 mm/ID 5.6 mm, 38 mm catalyst bed, 15 ml/min, 30 wt% MoO_3/γ-Al_2O_3. Averaged periodic profile (3_PP): PA 15%, PL 93 s, profile time span 3 h, XRD exposure time 1 s, 180 patterns averaged. Steady state profile (1_SS): profile time span 8 h, exposure time 60 s, 15 patterns averaged. Beamline P07: Beam size 0.5×0.5 mm^2 (h×v), 103.413 keV (λ = 0.1199 Å).

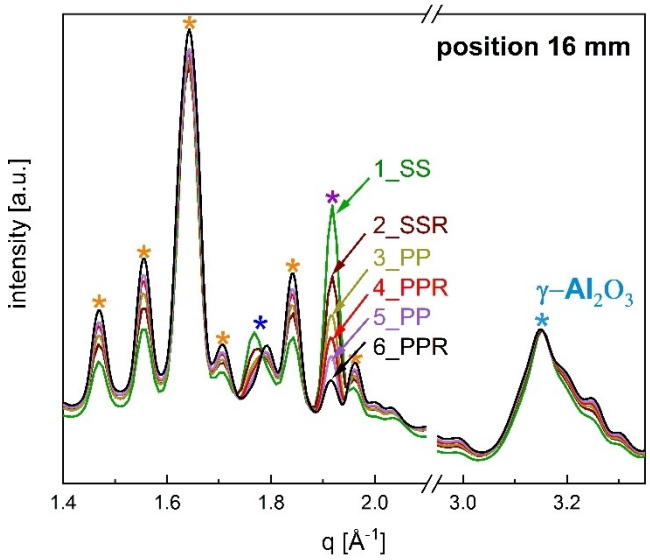

Figure 11. Averaged XRD patterns measured at position 16 mm of all six profile runs. Diffractograms are each normalized to the maximum signal at 3.15 $Å^{-1}$. Reaction conditions: Inlet composition C_2H_6/O_2:10/10, 515 °C, 1 bar, OD 6 mm/ID 5.6 mm, 38 mm catalyst bed, 15 ml/min, 30 wt% MoO_3/γ-Al_2O_3. Averaged periodic profiles: Profile time span 3 h, XRD exposure time 1 s, 180 patterns averaged, 3_PP/4_PPR: PA 15%/PL 93 s, 5_PP/6_PPR: PA 38%/PL 91 s. Steady state profiles (1_SS, 2_SSR): Profile time span 8 h, XRD exposure time 60 s, 15 patterns averaged. Beamline P07: Beam size 0.5×0.5 mm^2 (h×v), 103.413 keV (λ = 0.1199 Å).

can be compared with respect to signal to background ratio, positions and relative intensities in dependence of the profile runs. In this way, an increasing trend in intensity of signals at 1.47, 1.55, 1.64, 1.71, 1.84, 1.97 $Å^{-1}$ (orange asterisk, Figure 11), and a decreasing intensity at 1.92 $Å^{-1}$ (purple asterisk, Figure 11) are revealed in sequence with the profile runs from 1 to 6. Furthermore, a change in peak position from 1.77 to 1.79 $Å^{-1}$ (blue asterisk, Figure 11), as well as a change in its shape are observed.

The only decreasing reflection at 1.92 $Å^{-1}$ could be assigned to a stoichiometric molybdenum oxide (MoO_3) [ICDD No-. 98-064-4065], while the increasing reflection at 1.84 $Å^{-1}$ might originate from a formed stoichiometric MoO_2 [ICDD No-. 98-008-0830] phase, both confirming continuous catalyst reduction. In combination, a decreasing signal to background ratio suggests formation of XRD amorphous molybdenum suboxide phases. Further increasing peak intensities indicate a growing crystallite size or number of molybdenum oxides crystals, as previously seen in Figure 10. Overall, the profiles have a clear trend with increasing time of process operation and reveal pronounced structural changes in the catalyst bulk with time, most likely due to slow catalyst reduction processes. These observations provide evidence that the catalyst was not yet in steady state, even though catalytic performance was overall stable. While the extent of reduction is thermodynamically controlled in response to the local temperature and gas phase composition, the rate is determined by complex solid state kinetics, including slow oxygen diffusional processes from the bulk to near surface regions.[28,29] Therefore, bulk structural changes resulting from catalyst reduction occur at larger time scales of hours to reach steady state, as seen by the changes in the patterns in Figure 11.

Furthermore, solid oxygen diffusion at reactor scale might be a potential explanation of the rather long 6 mm phase transition zone, occurring in all profiles after the point of full oxygen conversion (18–24 mm). This zone is sandwiched between the first and third reactor region. The first region consists of various phases of molybdenum oxides MoO_{3-x} ($x \leq 1$) with a higher oxygen to metal ratio compared to the third region, which contains a stoichiometric MoO_2 phase. This stoichiometry variation may induce a gradient or driving force in the catalyst for oxygen diffusion, broadening the range of phase transition from 18 to 24 mm.

Applicability of the CPR for *operando* spatiotemporally-resolved catalysis studies

Overall, six profile runs were obtained within a short measurement time of 28 h, providing simultaneous information of local temperature, concentration, and structural XRD information of the catalyst under steady state and dynamic reaction conditions, statistically complemented with replicate runs. The accessible long and uniform heated catalyst bed zone of 38 mm allowed to probe the catalyst structure under strongly varying local gas compositions, and thus increasing the achievable information content within one profile run. Combined with fast setup assembly, enabled by the compact and integrated CPR design, the full potential of synchrotron studies can be exploited, which are typically restricted in measurement time and flexible accessibility. This demonstrates the power of spatial profiling using the CPR in systematic catalytic studies, providing a large amount of high quality information, considering different parts of the chemical system, in short measurement times under various reaction conditions. This offers a wide application range in future catalysis research, required to establish dynamic catalytic reactor operation at larger scale. As shown in this work, wide parameter fields can be screened to identify ranges for stable catalytic performance in a dynamic operation mode. Additionally, *operando* profile measurements are a promising approach to understand the long-term catalyst stability of dynamic catalyst systems and the resulting impact of changing catalyst structures on product yields. In both cases, the causes and symptoms of long-term structural changes are otherwise difficult to deduce based only on integral end-of-pipe measurements. Finally, *operando* periodic profile measurements allow for fast determination of dynamic operation conditions that enable improved catalytic performance in non-linear reaction systems, and to understand the underlying chemical processes involved.

Conclusion

The catalytic profile reactor setup is a versatile tool for highly complex *operando* measurements. It enables simultaneous

acquisition of spatiotemporally-resolved catalyst activity (gas composition and temperature) and structural information under a wide range of well-defined reaction conditions. In this study, the operation mode of the catalytic profile reactor setup was further extended from steady state to periodic conditions, using a sinusoidal inlet feed. The periodic profile methodology was tested in a catalytic performance study combined with kinetic modeling and with *operando* measurements using high-energy XRD. Ethane ODH over a MoO_3/γ-Al_2O_3 catalyst was used as a comparatively simple reaction system for the purposes of method development.

Process automation was successfully achieved utilizing the reactor control system. Simulative and experimental concentration profiles show stable catalytic performance under periodic reaction conditions with constant averaged target variables (conversion, selectivity), compared to steady state. Combined spatiotemporally-resolved *operando* XRD complements results with stable crystalline phases within short time periods of minutes. Distinct structural changes showing catalyst reduction are observed in space caused by strongly varying gas compositions along the catalyst bed (full oxygen conversion). Catalyst reduction is further seen at larger time scales of hours per position, whether at steady state or periodic conditions. Profile reactor operation under dynamic conditions coupled to time-resolved gas and structural analysis demonstrates its strengths in enhancing the information obtained from profile measurements compared to steady state operation, in this case by tracking chemical evolution of transient processes and application of a wider concentration range. Obtained profile results allow to identify improving, worsening, or constant catalytic performance under dynamic reaction conditions combined with detailed information of underlying processes.

Setup operation conditions include a broad and challenging range of feasible reaction parameters (e.g., reaction temperature: 515–550 °C, trace heating: 200 °C, pressure: 1–20 bar), allowing for probing numerous heterogeneously catalysed gas-solid or gas-liquid-solid reaction systems. In combination, high setup compatibility with a range of characterization techniques, such as XRD, XAS and Raman spectroscopy, as well as beamline integration at several absorption (P64/P65 PETRA III, DESY; ROCK, Soleil) and scattering (P07/P21.1 PETRA III, DESY) beamlines, strongly encourage deepened investigations of industrially relevant reaction systems in future studies.

Overall, the catalytic profile reactor setup is introduced as a useful tool for combined spatial profile studies in modern *operando* catalysis research. It is capable of being operated under various and dynamic reaction conditions. The compact design allows straightforward and fast experimental setup, enabling advanced catalytic studies, combined at laboratory or synchrotron radiation facilities, enhancing quality and reproducibility for interdisciplinary catalysis research studies for systematic development of improved catalytic processes.

Experimental Section

Experimental setup

In this work, catalyst investigation involves two parts. First, catalyst activity was studied by concentration profile measurements at steady state and periodic reactor operation. The measured periodic profiles were complemented with transient reactor simulations. Second, the developed periodic spatial profiling methodology was combined with catalyst characterization using spatiotemporally-resolved *operando* XRD. In all measurements ethane ODH on a 30 wt% MoO_3 supported on γ-Al_2O_3 catalyst with a particle size of 300–400 μm was used as a test reaction system. Catalyst preparation is reported elsewhere.[15] All experiments were conducted using the flexible setup configuration illustrated in Figure 12. The main setup parts consisted of: (i) gas dosing system; (ii) profile reactor; (iii) gas analytics; and (iv) characterization technique.

(i) Periodic reactor operation was performed by dosing the reactants in a sinusoidal manner, using a set of MFCs (Bronkhorst GmbH). Periodic variables (PS, PA, PL) of individual species could be modulated in relation to each other, while maintaining fairly constant total volumetric flow rates through the reactor with variations less than 4%. This was realized using the CPR control system, further illustrated in the reactor simulation subsection below.

(ii) Spatial and temporal gradients within the catalytic fixed bed were obtained by the CPR (REACNOSTICS GmbH), which utilizes the capillary sampling technique. The working principle of this technique is illustrated in Figure 13.

Here, the catalyst bed is fixed in position with quartz glass wool inside a fused silica reaction tube (OD 6 mm, ID 4–5.6 mm), vertically mounted to prevent bypass flows. A stainless steel capillary (OD 700 μm, ID 520 μm) sits in the center of the catalyst bed with a sheath-thermocouple type K (OD 250 μm, TMH GmbH), using Inconel as sheath material, located within. The capillary has four side sampling orifices (75 μm), laser drilled and arranged with an angular offset of 90° at the same axial position (LaserMicronics GmbH), through which small gas samples are continuously extracted. The tip of the thermocouple and the position of the sampling orifices are aligned with the optical access window(s) of the CPR. Uniform sample heating up to 515 °C using an oven, as

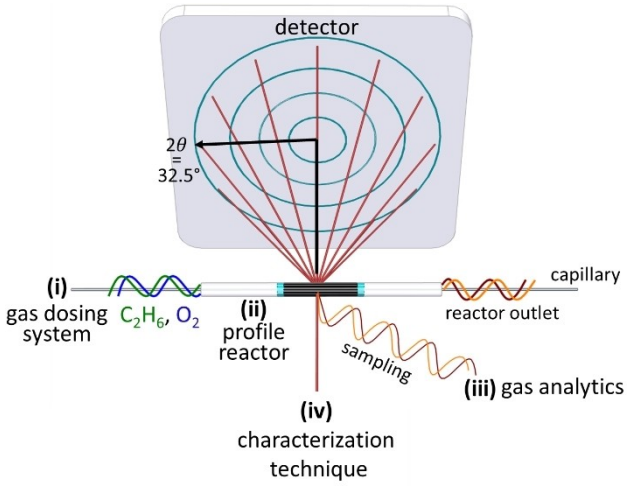

Figure 12. Schematic overview of the experimental setup used for catalytic performance and *operando* spatial and temporal profile studies. (i) Gas dosing; (ii) profile reactor; (iii) gas analytics; (iv) characterization technique.

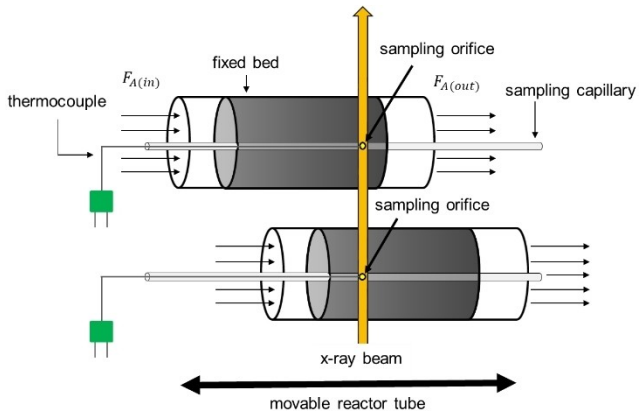

Figure 13. Working principle of the spatial profile measurement technique.

well as trace heating up to 200 °C, including transfer lines (Hillesheim GmbH) and the interior of the reactor, are achieved. Reaction gases were preheated to the target temperature through a 4 cm long preheating zone. Local measurements are therefore possible up to 5.5 cm long catalyst bed. For a detailed description of the profile technique the reader is referred to our previous work.[15] Different CPR types were developed based on the individual characterization technique and reaction condition requirements. Here, the synchrotron CPR-XRD is used, allowing measurements with a solid angle of 2θ up to 32°.

(iii) In order to analyse periodic reactor operation in terms of catalyst performance, fast data acquisition is required. Thus, gas analysis was performed by a mass spectrometer (MS, Hiden HPR 20), equipped with a Faraday cup and a heated capillary inlet. To reduce the measurement time only specific mass to charge ratios (m/z) were scanned: ethylene 27, ethane 30, oxygen 32, argon 40. Signal contribution of ethane fragments to the peak at 27 were subtracted prior ethylene quantification. The scan was taken in Multiple Ion Detection (MID) mode, acquiring the maximum intensity at a chosen mass. Gas quantification of ethane, ethylene and oxygen was carried out using the internal standard method and dosing known reaction mixtures. To ensure small sampling flow rates of approximately 5% of the total flow rate through the CPR, a micrometer needle valve (Vici Valco GmbH) was used and heated by a heating jacket (Horst GmbH). Small sampling flow rates are important to reduce the invasiveness of the sampling methodology on hydrodynamic conditions within the reactor. Overall, the heated system makes measurements of easily condensable reactants feasible.

Operando high-energy XRD

Spatiotemporally-resolved *operando* catalyst characterization (iv) was performed by means of high-energy XRD at beamline P07 of the PETRA III storage ring at Deutsches Elektronen-Synchrotron (DESY) in Hamburg, Germany. The incident X-ray energy was set to 103.6 keV, λ = 0.1199 Å. The application of high energies minimized diffraction angles according to Bragg's law of diffraction which allows to record a large part of reciprocal space through the sample window in the reactor back and made beam attenuation negligible. To minimize signal contributions from fused silica in the XRD patterns, a thin-walled reaction tube (OD 6.0 mm, ID 5.6 mm) was used. Patterns were acquired in a small q range from 1.3–11 $Å^{-1}$. The beam was aligned next to the capillary and beam size was reduced and square-shaped by slits to 0.5 × 0.5 mm^2 to prevent hitting the stainless steel capillary during translation of the reactor bed. The alignment of the thermocouple tip with the orifice and beam position was determined via an X-ray eye,[30] resulting in deviations of 1.6 mm at reaction conditions. At each sample position an automated measurement script was started by the reactor control system. Scripts for steady state profiles took first a dark image and afterwards 15 sample images with an exposure time of 60 s each, while periodic profiles recorded 180 diffractograms with an exposure time of 1 s each. Diffraction patterns were acquired using a 2D 432 × 432 mm^2 Varex Imaging XRD 4343CT detector with a pixel size of 150 × 150 μm^2. A sample to detector distance of 1170 mm was obtained through calibration of the Debye-Scherrer rings using CeO_2 as standard. Azimuthal integration was performed using the pyFAI package.[31] Further qualitative phase analysis was performed by the Highscore Plus software,[32] using the crystallographic data file from MoO_2 (ICDD No-. 98-015-2316).

Reactor simulations

Catalyst performance under periodic conditions was explored by reactor simulations over a broad range of periodic reaction conditions. A kinetic model, previously developed for the applied test reaction system at steady state,[15] was used and extended to periodic reaction conditions using COMSOL Multiphysics 5.5. A one-dimensional pseudo-homogeneous packed bed reactor model with constant density, constant temperature and constant pressure was used. This plug flow model only considers transport by convection, and thus concentration gradients only in axial direction. The steady state reactor model is shown in Equation (2) for one component *i*. The weight based net reaction rate $r_{i,\,net}$ of consumption/production is calculated by considering species transport through convection by the molar concentration as function of the position along the catalyst bed *dz*, the bed density ρ_{bed} and the gas velocity u_z in axial direction.

$$r_{i,\,net} * \rho_{bed} = \frac{dc_i}{dz} * u_z \tag{2}$$

Transient plug flow behaviour was modeled adding the time dependency of component *i*.

$$r_{i,\,net} * \rho_{bed} = \frac{\partial c_i}{\partial t} + \frac{\partial c_i}{\partial z} * u_z \tag{3}$$

Periodic inlet feed for one reactant component *i* (e.g. ethane, oxygen) was simulated using Equation (4). Here, $\dot{V}_{i,SS}$ represents the volumetric flow at steady state conditions of component *i*, from which the oscillation starts. The resulting periodic flow rate for the component $\dot{V}_{i,\,PP}$ is obtained by multiplying a unit base sinusoidal function, defined by the periodic variables PA, PL, PS and the time *t*, with $\dot{V}_{i,SS}$.

$$\dot{V}_{i,\,PP(t)} = \dot{V}_{i,SS}\left(1 + PA_i * \sin\left(\left(\frac{2^* \pi}{PL_i}\right) * t + PS_i\right)\right) \tag{4}$$

$\dot{V}_{i,SS}$ is related with the *average* volume fraction of component *i*, $\bar{f}_i$, via Equation (5) and (6). Here, the periodic volumetric flow of component *i* is averaged at position 0 mm (inlet flow) and divided by the total flow rate $\dot{V}_{tot}$.

$$\dot{V}_{i,SS} = \bar{f}_i * \dot{V}_{tot} \tag{5}$$

$$\bar{f}_i = \frac{\sum_{t=0}^{n} \dot{V}_{i,\,PP(t;0mm)}}{n^* \dot{V}_{tot}} \quad (6)$$

Finally, Equation (3) is solved for each reactant component, which should fluctuate periodically, while the inert flow is adapted according to $\dot{V}_{i,\,PP}$ for keeping a constant total flow rate through the reactor, represented by $\dot{V}_{tot}$. In Figure 14, this is exemplarily shown for a total flow rate of 40 ml/min, an inlet composition of O_2/C_2H_6/inert:10/10/80 and the periodic variables PA 10%, PS 180° and PL 60 s. An average volumetric feed composition of 10 vol% and a PA of 10% corresponds to a O_2 or C_2H_6 fluctuation of 3.6 (minimum) to 4.4 ml/min (maximum). Furthermore, a PS describes the shift in between the two components, and is thus only present if two components are varied at the same time. Optimization was performed using a parametric sweep of all periodic variables in a range of PS: 0–180°, PA: 5–35%, PL: 0.01–60 s.

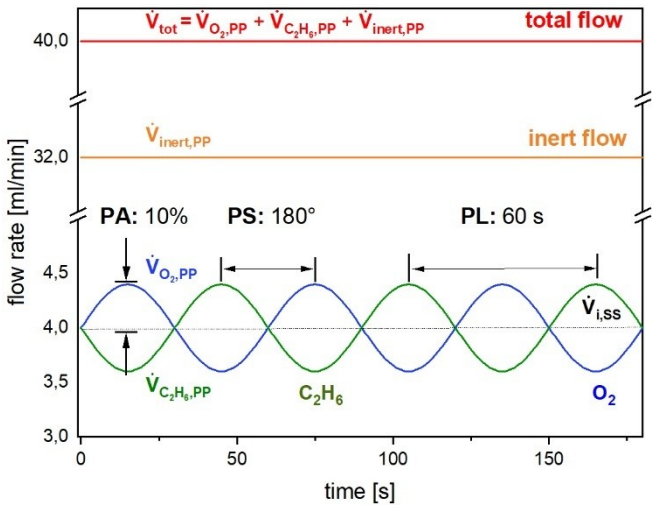

Figure 14. Schematic representation of the periodic reactor control together with its operating variables PA, PS and PL.

Overview profile experiments

In Table 1 an overview of the experimental reaction conditions is given, divided into catalytic performance (1st experimental part) and *operando* XRD experiments (2nd experimental part). Overall, two profiles were measured in the catalytic performance study, consisting of one steady state (CP_SS) and one periodic (CP_PP) profile. During *operando* XRD three profiles with one additional replicate profile each (in total six profiles) were conducted. The *operando* steady state profiles are denoted as 1_SS and 2_SSR. During one periodic profile set (3_PP, 4_PPR) oxygen was oscillated, and in the other one (5_PP, 6_PPR) ethane. Notably, the simultaneously measured concentration profiles are not presented in this work since no additional information of higher value is gained compared to the 1st experimental part.

Acknowledgements

The authors thank Martin Böttcher from Reacnostics GmbH for modifying the profile reactor. We acknowledge DESY (Hamburg, Germany), a member of the Helmholtz Association HGF, for the provision of experimental facilities. Parts of this research were carried out at PETRA III using the photon beamline P07. Beamtime was allocated for proposal I-20010075. This work was supported by the German Federal Ministry of Education and Research (BMBF) project COSMIC (no. 05K19GT1 Hamburg University of Technology, no. 05K19VK4 Karlsruhe Institute of Technology). We also thank Christina Laarmann for producing the catalyst used in this work and Alana Sá for supporting the catalytic performance studies. Open Access funding enabled and organized by Projekt DEAL.

Conflict of Interest

The authors declare no conflict of interest.

Table 1. Overview of the experimental conditions used for catalytic performance and *operando* spatial and temporal profile studies. PA is varied around the steady state inlet composition of ethane or oxygen, respectively. PS refers to a shift in between the reactants oxygen and ethane.

Experimental Parameters	Catalyst performance	*Operando* XRD
Reactor tube diameter [mm]	OD 6.0, ID 4.0	OD 6.0, ID 5.6
Catalyst	30 wt% MoO_3/γ-Al_2O_3	
Flow rate [ml/min]	40	15
Temperature [°C]	515	515
Pressure [bar]	1	1
Inlet composition at steady state C_2H_6/O_2/inert **[vol%]**	10/10/80	10/10/80
Average at periodic C_2H_6/O_2/inert **[vol%]**	10/10/80	10/10/80
PA [%]	CP_PP: C_2H_6:9, O_2:5	3_PP/4_PPR: 15 5_PP/6_PPR: 38
PS [°]	180	–
PL [s]	95	3_PP/4_PPR: 93 5_PP/6_PPR: 91
Catalyst bed length [mm]	32	38
Maximum O_2 conversion [%]	42	100
Measurement time per profile	SS: 1.5 h PP: 1.5 h	SS: 8 h PP: 3 h
Scanned m/z ratios	27, 30, 40	27, 30, 32, 40

Data Availability Statement

The data that support the findings of this study are available from the corresponding author upon reasonable request.

Keywords: heterogeneous catalysis · kinetic modeling · periodic reactor operation · spatiotemporal *operando* study · X-ray diffraction

[1] a) P. Lemke, J. F. Ren, R. Alley, I. Allison, J. Carrasco, G. Flato, Y. Fujii, G. Kaser, P. Mote, R. Thomas et al. in *IPCC*, **2007**; b) M. Buck, A. Graf, P. Graichen, *European Energy Transition 2030: The Big Picture. Ten Priorities for the next European Commission to meet the EU's 2030 targets and accelerate towards 2050*, **2019**.
[2] K. F. Kalz, R. Kraehnert, M. Dvoyashkin, R. Dittmeyer, R. Gläser, U. Krewer, K. Reuter, J.-D. Grunwaldt, *ChemCatChem* **2017**, *9*, 17.
[3] L. Grajciar, C. J. Heard, A. A. Bondarenko, M. V. Polynski, J. Meeprasert, E. A. Pidko, P. Nachtigall, *Chem. Soc. Rev.* **2018**, *47*, 8307.
[4] X. Shi, X. Lin, R. Luo, S. Wu, L. Li, Z.-J. Zhao, J. Gong, *JACS Au* **2021**, *1*, 2100.
[5] a) M. A. Bañares, *Catal. Today* **2005**, *100*, 71; b) J. Frenken, *Operando Research in Heterogeneous Catalysis*, Springer International Publishing, Cham, **2017**; c) H. Topsøe, *J. Catal.* **2003**, *216*, 155.
[6] a) A. Gaur, M. Schumann, K. V. Raun, M. Stehle, P. Beato, A. D. Jensen, J.-D. Grunwaldt, M. Høj, *ChemCatChem* **2019**, *11*, 4871; b) S. Müller, A. Zimina, R. Steininger, S. Flessau, J. Osswald, J.-D. Grunwaldt, *ACS Sens.* **2020**, *5*, 2486.
[7] a) S. Alizadehfanaloo, J. Garrevoet, M. Seyrich, V. Murzin, J. Becher, D. E. Doronkin, T. L. Sheppard, J. D. Grunwaldt, C. G. Schroer, A. Schropp, *J. Synchrotron Radiat.* **2021**, *28*, 1518; b) S.-C. Lin, C.-C. Chang, S.-Y. Chiu, H.-T. Pai, T.-Y. Liao, C.-S. Hsu, W.-H. Chiang, M.-K. Tsai, H. M. Chen, *Nat. Commun.* **2020**, *11*, 3525; c) A. S. M. Ismail, I. Garcia-Torregrosa, J. C. Vollenbroek, L. Folkertsma, J. G. Bomer, T. Haarman, M. Ghiasi, M. Schellhorn, M. Nachtegaal, M. Odijk et al., *ACS Catal.* **2021**, *11*, 12324.
[8] F. Bonino, E. Groppo, C. Prestipino, G. Agostini, A. Piovano, D. Gianolio, L. Mino, E. Gallo, C. Lamberti in *Synchrotron Radiation* (Eds.: S. Mobilio, F. Boscherini, C. Meneghini), Springer Berlin Heidelberg, Berlin, Heidelberg, **2015**, pp. 717–736.
[9] T. Günter, D. E. Doronkin, H. W. P. Carvalho, M. Casapu, J.-D. Grunwaldt, *J. Phys. Conf. Ser.* **2016**, *712*, 012071. .
[10] a) A. M. Beale, A. M. J. van der Eerden, K. Kervinen, M. A. Newton, B. M. Weckhuysen, *Chem. Commun. (Cambridge, U. K.)* **2005**, 24, 3015; b) K. H. Cats, B. M. Weckhuysen, *ChemCatChem* **2016**, *8*, 1531; c) F. Meirer, B. M. Weckhuysen, *Nat. Rev. Mater.* **2018**, *3*, 324.
[11] a) J. Touitou, R. Burch, C. Hardacre, C. McManus, K. Morgan, J. Sá, A. Goguet, *Analyst* **2013**, *138*, 2858; b) F. Wolke, Y. Hu, M. Schmidt, O. Korup, R. Horn, E. Reichelt, M. Jahn, A. Michaelis, *Catal. Commun.* **2021**, *158*, 106335.
[12] a) J. Becher, D. F. Sanchez, D. E. Doronkin, D. Zengel, D. M. Meira, S. Pascarelli, J.-D. Grunwaldt, T. L. Sheppard, *Nat. Catal.* **2021**, *4*, 46; b) J. Becher, S. Weber, D. Ferreira Sanchez, D. E. Doronkin, J. Garrevoet, G. Falkenberg, D. Motta Meira, S. Pascarelli, J.-D. Grunwaldt, T. L. Sheppard, *Catalysts* **2021**, *11*, 459; c) J.-D. Grunwaldt, B. Kimmerle, A. Baiker, P. Boye, C. G. Schroer, P. Glatzel, C. N. Borca, F. Beckmann, *Catal. Today* **2009**, *145*, 267; d) F. Maurer, J. Jelic, J. Wang, A. Gänzler, P. Dolcet, C. Wöll, Y. Wang, F. Studt, M. Casapu, J.-D. Grunwaldt, *Nat. Catal.* **2020**, *3*, 824.
[13] a) M. Geske, O. Korup, R. Horn, *Catal. Sci. Technol.* **2013**, *3*, 169; b) M. Wolf, N. Raman, N. Taccardi, R. Horn, M. Haumann, P. Wasserscheid, *Faraday Discuss.* **2021**, *229*, 359.
[14] a) D. Decarolis, A. H. Clark, T. Pellegrinelli, M. Nachtegaal, E. W. Lynch, C. R. A. Catlow, E. K. Gibson, A. Goguet, P. P. Wells, *ACS Catal.* **2021**, *11*, 2141; b) C. Stewart, E. K. Gibson, K. Morgan, G. Cibin, A. J. Dent, C. Hardacre, E. V. Kondratenko, V. A. Kondratenko, C. McManus, S. Rogers et al., *ACS Catal.* **2018**, *8*, 8255.
[15] B. Wollak, D. E. Doronkin, D. Espinoza, T. Sheppard, O. Korup, M. Schmidt, S. Alizadefanaloo, F. Rosowski, C. Schroer, J.-D. Grunwaldt, R. Horn, *J. Catal.* **2021**, *408*, 372.
[16] M. A. Newton, S. Checchia, A. J. Knorpp, D. Stoian, W. van Beek, H. Emerich, A. Longo, J. A. van Bokhoven, *Catal. Sci. Technol.* **2019**, *9*, 3081.
[17] J. Touitou, F. Aiouache, R. Burch, R. Douglas, C. Hardacre, K. Morgan, J. Sá, C. Stewart, J. Stewart, A. Goguet, *J. Catal.* **2014**, *319*, 239.
[18] Y. Dong, M. Geske, O. Korup, N. Ellenfeld, F. Rosowski, C. Dobner, R. Horn, *Chem. Eng. J.* **2018**, *350*, 799.
[19] P. L. Silveston, R. R. Hudgins, *Periodic operation of reactors*, Elsevier, Oxford, **2013**.
[20] a) F. Cavani, N. Ballarini, A. Cericola, *Catal. Today* **2007**, *127*, 113; b) "Oxidative Dehydrogenation of Alkanes": S. F. Håkonsen, A. Holmen in *Handbook of Heterogeneous Catalysis*, Wiley-VCH, **2008**. .
[21] C. Baroi, A. M. Gaffney, R. Fushimi, *Catal. Today* **2017**, *298*, 138.
[22] D. Creaser, B. Andersson, R. R. Hudgins, P. L. Silveston, *Chem. Eng. Sci.* **1999**, *54*, 4437.
[23] a) J. Haber in *Stud. Surf. Sci. Catal.*, Elsevier, **1997**, pp. 1–17; b) J. Haber, E. M. Serwicka, *React. Kinet. Catal. Lett.* **1987**, *35*, 369.
[24] J. Haber in *Handbook of Heterogeneous Catalysis* (Eds.: G. Ertl, H. Knözinger, F. Schüth, J. Weitkamp), Wiley-VCH Verlag GmbH & Co. KGaA, Weinheim, Germany, **2008**.
[25] a) C. A. Gärtner, A. C. van Veen, J. A. Lercher, *ChemCatChem* **2013**, *5*, 3196; b) P. Mora-Briseño, G. Jiménez-García, C.-O. Castillo-Araiza, H. González-Rodríguez, R. Huirache-Acuña, R. Maya-Yescas, *Int. J. Chem. React. Eng.* **2019**, *17*, 20180085.
[26] a) D. E. Mears, *Ind. Eng. Chem. Process Des. Dev.* **1971**, *10*, 541; b) D. E. Mears, *J. Catal.* **1971**, *20*, 127.
[27] M. Dieterle, *Dissertation*, Technische Universität Berlin, Berlin, **2001**.
[28] T. Ressler, R. E. Jentoft, J. Wienold, M. M. Günter, O. Timpe, *J. Phys. Chem. B* **2000**, *104*, 6360.
[29] T. Ressler, *J. Catal.* **2002**, *210*, 67.
[30] W. Rischau, *Characterization of the X-ray eye*, DESY Summer School, **2009**.
[31] J. Kieffer, V. Valls, N. Blanc, C. Hennig, *J. Synchrotron Radiat.* **2020**, *27*, 558.
[32] T. Degen, M. Sadki, E. Bron, U. König, G. Nénert, *Powder Diffr.* **2014**, *29*, S13–S18.

Manuscript received: March 9, 2022
Revised manuscript received: October 18, 2022
Accepted manuscript online: October 24, 2022
Version of record online: November 22, 2022